Adaptive Hosking Generator with Time-Varying Hurst for HRV Simulation in Support of Digital Twin Modeling

Galya Georgieva-Tsaneva
Institute of Robotics
Bulgarian Academy of Science
Sofia, Bulgaria
galitsaneva@abv.bg

***Abstract*—This paper proposes an adaptive Hosking-type generator for simulating heart rate variability (HRV) with a time-varying Hurst exponent (t). Building on the classical Durbin-Levinson (Hosking) framework for fractional Gaussian noise (fGn), the new method allows for both segmental and online control of $H(t)$) to reproduce realistic transitions between rest, exercise, and recovery; introduces local anchoring of physiological metrics by matching SDNN and RMSSD moments in sliding windows; and provides seamless transitions between moment-matched modes (mean and variance) to avoid artifacts. The approach is validated using local estimates of the Hurst parameter and SDNN/RMSSD target coherence. Demonstrations show robust tracking of set targets across segments and smooth, jump-free transitions in the first two moments. The method is computationally efficient and suitable for real-time use, algorithm testing, and scenario-driven modeling in sports and clinical cardio-monitoring settings.**

Keywords— heart rate variability; Hosking algorithm; time-varying Hurst exponent; fractional Gaussian noise; moment matching; SDNN; RMSSD; adaptive simulation; DFA; sports physiology.

I. INTRODUCTION

Heart rate variability (HRV) is a well-established noninvasive marker of autonomic regulation, recovery, and stress. Normal RR intervals have been shown to exhibit self-similarity and long-term correlation memory, characteristic of fractal processes. Quantification is often performed using the Hurst exponent (H), as well as classical metrics such as SDNN and RMSSD, which reflect long-term and short-term variability, respectively.

Existing approaches to HRV simulation are typically either spectrally-based or based on fractional Gaussian noise/Brownian motion (fGn/fBm) with constant H. This limits the ability to realistically simulate dynamic transitions between physiological states (e.g., from rest to exercise to recovery), where statistical parameters and measures of self-similarity change over time. At the same time, there is no generally accepted single methodology for reliable estimation of H, and the generation of synthetic data with controlled transitions and target metrics remains an open research question.

The Hosking algorithm (Durbin–Levinson recursion) allows for the accurate generation of Gaussian processes with arbitrarily set autocovariance. For fGn, this autocovariance is an analytic function of H, making Hurst a natural control parameter of the simulator. However, the classical use with a constant H does not capture the transitions between physiological states and often introduces artifacts when trying to create segments with different variability parameters.

In this work, an adaptive Hosking generator for HRV with segmental time-varying H(t) is presented, attempting to solve the issue of smooth transition between individual modes, with the aim of working on online control towards target SDNN/RMSSD in the future. The main idea is to set modes (rest, load, recovery) with different values of H, with the transitions being implemented through cross-fade and moment matching (mean and variance) to avoid abrupt transitions from one state to another. Additionally, local sliding window control is applied to bring SDNN/RMSSD closer to realistic targets without disturbing the global fractal structure.

The presented approach provides realistic, labeled synthetic data for training and validation of algorithms (detection of stress, fatigue, dysfunction, etc.). The module can serve as a simulation layer in a digital twin of HRV, allowing personalized "what-if" scenarios and assessment of the response to training/recovery while maintaining confidentiality (without sharing raw patient data).

Contributions of the study:

1. An adaptive Hosking algorithm with time-varying H(t) (segmentally or in the form of a profile) is proposed.
2. We introduce seamless stitching via cross-fade with moment match, which eliminates artifacts in transitions.
3. A diagnostic toolkit is used: sliding metrics, Poincaré diagrams (SD1/SD2) and recurrence plots for comparable assessment between modes.
4. Applicability for customized simulations and tests in the context of a digital twin of HRV is demonstrated.

II. BACKGROUND

Heart rate variability is a standard indicator of autonomic regulation and risk, with definitions and measurement methods established by the ESC/NASPE Task Force (Task Force, 1996) [1]. The document provides recommendations for the determination of temporal, frequency, and geometric indices and is a starting point for assessing HRV.

ACKNOWLEDGE THE FINANCIAL SUPPORT OF THE PROJECT WITH FINANCING AGREEMENT NO. PVU-44 OF 05.12.2024 UNDER PROJECT NO. BG-RRP-2.017-0011 "ECOLOGICAL COLLABORATIVE ROBOTS POWERED BY GREEN HYDROGEN" UNDER THE RECOVERY AND RESILIENCE MECHANISM FOR THE IMPLEMENTATION OF AN INVESTMENT UNDER C2I2 "INCREASING THE INNOVATION CAPACITY OF THE BULGARIAN ACADEMY OF SCIENCES (BAS) IN THE FIELD OF GREEN AND DIGITAL TECHNOLOGIES" FROM THE RECOVERY AND RESILIENCE PLAN, BULGARIA.

HRV signals exhibit self-similarity and long-term correlations, described by fractal parameters and the Hurst exponent H [2]. To accurately generate Gaussian processes with a predetermined autocovariance, the Hosking algorithm (Durbin–Levinson recursion) is used [3]. In fractional Gaussian noise (fGn), the autocovariance is an analytic function of H, so H becomes a natural input parameter of the generator. Hosking's original work and related materials on Durbin–Levinson and Toeplitz structures are the main technical sources on this subject [4,5,6].

Poincaré plots (SD1/SD2) [7,8] are used to study the nonlinearity of HRV, which capture short-term versus long-term variability and relate it to physiological state.

Another research method is Recurrence Plots (RP) and Recurrence Quantification Analysis (RQA), which assess determinism, laminarity, and transitions between regimes [9,10].

Recent research articles and methodological reviews on nonlinear HRV analyses (including Poincaré/RP) in a clinical context—show the utility of HRV simulation methods [11,12,13].

III. Adaptive Hosking Generator for HRH with Time-Variating Hurst and Momentary Matching of Metrics

Let X_t be a stationary Gaussian process (fGn) with variance $\sigma^2$and Hurst H$\in$(0,1). The autocovariance is given by the formula:

$$\gamma_H(k) = \frac{\sigma^2}{2}(|k-1|^{2H} - 2|k|^{2H} + |k+1|^{2H}), k \geq 0 \quad (1)$$

Using Durbin–Levinson recursion, AR coefficients $\{\varphi_{n,j}\}$ and variance are determined v_n, after which one step of the process is generated:

$$X_{n+1} = \sum_{j=1}^{p} \varphi_{n,j} X_{n+1-j} + \varepsilon_{n+1} \quad (2)$$

$$\varepsilon_{n+1} \sim N(0, v_n), \quad (3)$$

$p \epsilon [10,30]$ – order of the process.

Creating a time-varying H(t)

The signal is divided into S segments $[t_{s-1}+1, t_s]$, each with a constant H_s. In each segment $\gamma_H(k)$ is used and X_t is generated using Hosking's algorithm.

The smooth transition from one segment to another in a zone of length C around the boundary t_s is realized by blending the end of segment s and the beginning of s+1:

$$\tilde{X}_t = \alpha_t X_t^{(s)} + (1-\alpha_t) X_t^{(s+1)} \quad (4)$$

$$\alpha_t = \frac{t_s - t + 1}{C}, \quad (5)$$

$$t \in [t_s - C + 1, t_s]. \quad (6)$$

Before mixing, it is performed:

$$X^{(\cdot)} \leftarrow \mu^* + \frac{\sigma^*}{\hat{\sigma}^{(\cdot)}}(X^{(\cdot)} - \hat{\mu}^{(\cdot)}) \quad (7)$$

$(\widehat{\mu}, \widehat{\sigma})$ are empirical moments in the window, and (μ^*, σ^*) – are target moments.

Matching SDNN and RMSSD. Working on a sliding window of RR intervals. Let R_t be an RR series with a desired mean μ_{RR}:

$$R_t = \bar{R} + s(R_i - \bar{R}), \quad (8)$$

$$i \in [t - W + 1, t], \quad (9)$$

$\bar{R}$ – average value in the window;

s – combination of two multipliers that change SDNN and RMSSD:

$$s_{SD} = \frac{SDNN^{target}}{\widehat{SDNN}}, s_{RM} = \frac{RMSSD^{target}}{\widehat{RMSSD}}, \quad (10)$$

$$s = \alpha . s_{SD} + (1-\alpha) s_{RM}, \alpha \in [0,1]. \quad (11)$$

where:

$$\widehat{SDNN} = \sqrt{\frac{1}{W-1}\sum_{i=2}^{W}(R_i - \bar{R})^2}, \quad (12)$$

$$\widehat{RMSSD} = \sqrt{\frac{1}{W-1}\sum_{i=2}^{W}(R_i - R_{i-1})^2}. \quad (13)$$

The proposed method locally corrects the amplitude while preserving the long-term correlation structure, using short windows and preserving the average $\bar{R}$.

IV. Rezults

The following 3 figures show the variable nature of the HRV and its two parameters in three simulated segments with different Hurst exponents. Figure 1 shows the simulated RR intervals in the individual sections, separated by a green vertical line. In the first section, the blue series passes through two green markers, with the average RR being longer at rest, shortening under load (increased heart rate) and gradually returning to higher values in recovery; the transitions are smooth thanks to cross-fade.

The resulting RR series is smooth and without jumps when changing modes, which confirms that cross-fade + match sometimes eliminate artifacts at the boundaries. The sliding SDNN and RMSSD reflect the change in self-similarity: in the middle segment (different H) a rearrangement of the short-term variability is clearly visible, followed by stabilization in recovery. The absolute values of the metrics here are small (demo without aggressive scaling), but the relative profile and smooth transitions show that the proposed scheme can controllably model rest–load–recovery scenarios and preserve the continuity of the first two moments – key for correct subsequent DFA/PSD-analyzis. If necessary, by momentary matching (target SDNN/RMSSD) we can set the levels to realistic clinical ranges without disturbing the evolution of H(t).

The Figure 2 (sliding SDNN, win=120) shows the expected profile: higher long-term variability at rest, reduction under load and partial recovery after the second marker. The Figure 3 (sliding RMSSD) reflects the short-term dynamics: lower values at rest, a clear drop at the beginning of the load and a gradual decrease after the peak, which is consistent with the recovery and damping of high-frequency oscillations. The overall result confirms that the adaptive Hosking generator with segmented H and seamless stitching reproduces realistic regime changes, preserving continuity and stable instantaneous characteristics.

The proposed model can simulate transient processes when studying the three physiological states of rest, exercise and recovery.

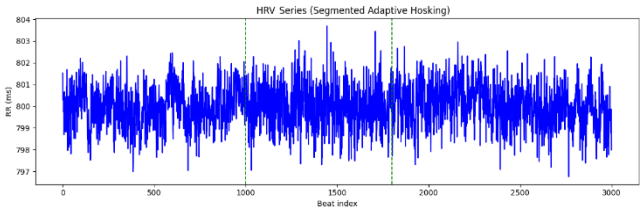

Fig. 1. Fig. 1. Synthetic RR sequence generated with a segmented Hosking model (3 segments).

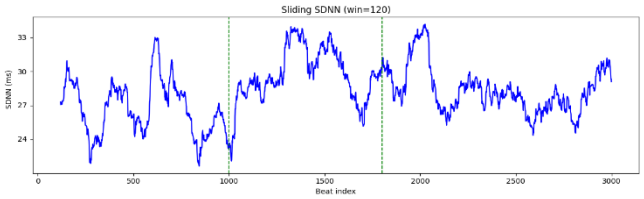

Fig. 2. Sliding SDNN window (3 segments).

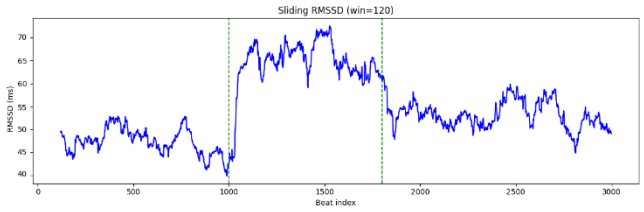

Fig. 3. Sliding RMSSD window (3 segments).

The following figures show the simulated graphs in 9 different segments (to demonstrate the possibility of simulating multiple segments with different Hurst exponents): the generated HSC is given in Figure 4; Figure 5 presents the SDNN of the series and Figure 6 shows the RMSSD values. The individual segments are separated by green vertical lines and have the following Hurst exponent values: 0.8; 0.6; 0.75; 0.8; 0.65; 0.7; 0.83; 0.62; 0.77. Figures 5 and 6 show that changes in the Hurst exponent lead to changes in the studied HSC parameters.

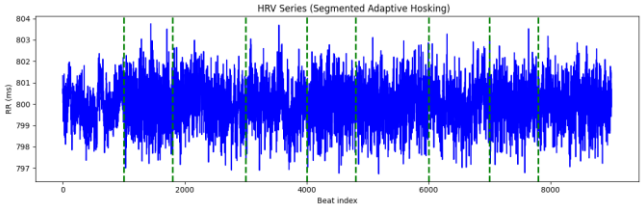

Fig. 4. Synthetic RR sequence generated with a segmented Hosking model (9 segments).

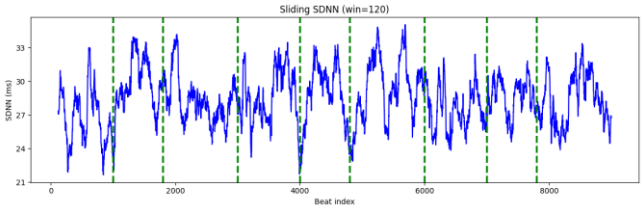

Fig. 5. Sliding SDNN window (9 segments).

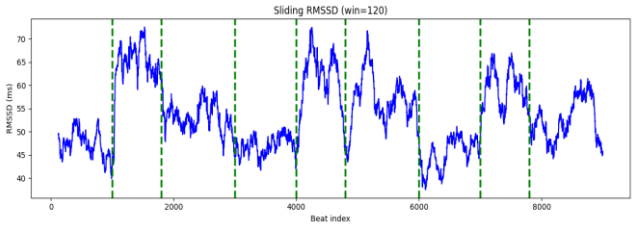

Fig. 6. Sliding RMSSD window (9 segments).

The three Recurrence Plots show a change in the dynamics of the VCH by mode. At rest (Figure 7: Segment 1) the matrix is denser with clearly outlined short diagonal chains, which indicates increased determinism and a more stable short-term structure (at higher H and slower rhythm). At load (Figure 8: Segment 2) the total recurrence decreases, the diagonal threads are rarer/shorter and more “noisy” points appear; the diagram shows more unstable transitions and a lower order in the oscillations (accelerated pulse, lower autocorrelation). At recovery (Figure 9: Segment 3) the density and lengths of the diagonals increase relative to the load, but remain below the rest level, with a gradual structuring in the middle part — a partial return of the order and memory of the process. These differences in RP (at fixed ε) coherently reflect segmental changes in μRR and H: greater determinism and recurrence at rest, reduction under load, and smooth recovery of correlation structures.

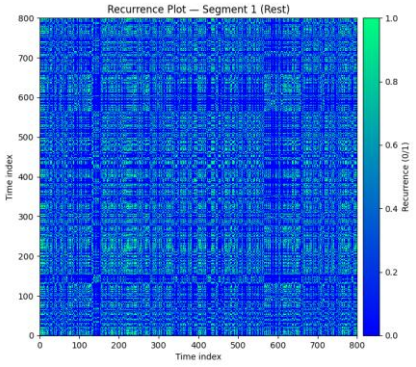

Fig. 7. Recurrence Plot (Segment 1).

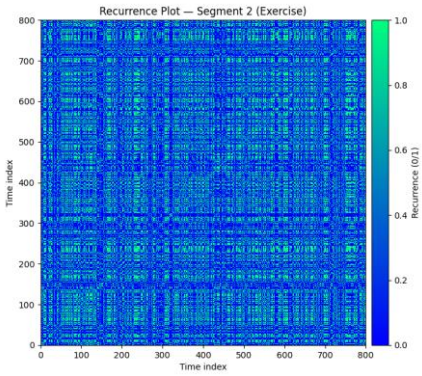

Fig. 8. Recurrence Plot (Segment 2).

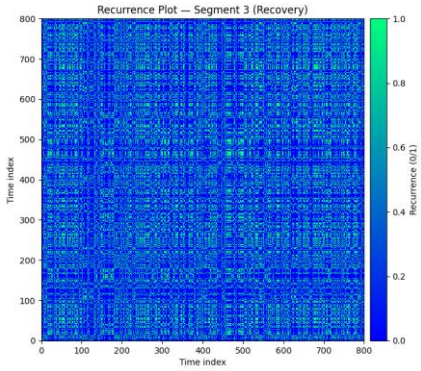

Fig. 9. Recurrence Plot (Segment 3).

Practical applications in a HRV Digital Twin

- Personalized "what-if" simulations. Ability to switch modes (rest, exercise, recovery) and analyze how SDNN/RMSSD, H(t), LF/HF would change under different training and stress situations.
- Calibration to a specific person. Estimating H(t), SDNN, RMSSD, etc. from real recordings and allowing the simulator to reproduce them. Creating a digital twin that matches the HRV parameters of the real athlete/patient.
- Generating synthetic data with labels. Creating large, controlled sets (rest/exercise/recovery) for training/validation of detectors for fatigue, stress, arrhythmias – with guaranteed target metrics and H(t).
- Real-time algorithm testing. Possibility to implement online control, where RR series are fed to detectors (DFA-based, LF/HF, etc.) to test stability, latency, thresholds without waiting for the actual session.
- Recovery and load assessment. Support optimal training planning: simulate high-interval training vs. volume session, compare expected RMSSD decline and H(t) recovery.
- Method robustness. Add controlled transitions and micro-artifacts; check which algorithm works or fails with a sharp shift in H(t) or low RMSSD.
- Boundary conditions and safety. Simulate extreme scenarios (dehydration, sleep deprivation) and study which combinations of H(t)/SDNN/RMSSD trigger an alarm.
- Privacy: Synthetic Twins. Create models and interfaces with non-identifying synthetic RRs that statistically match the patient without sharing raw data.
- Sensor/Telemetry Planning. Assess how down-sampling/losses affect local metrics; optimize buffers, compression, and data transmission thresholds.
- Visualize the "target" SDNN/RMSSD/H(t) curve and simulate how, for example, breathing exercises/rests would bring metrics back into the green zone.
- Compare across the same scenarios different stress/fatiue models, examining the impact of different factors.
- Integration into the digital twin as a simulation module layer.

ACKNOWLEDGMENT

THE AUTHOR ACKNOWLEDGES THE FINANCIAL SUPPORT OF THE PROJECT WITH FINANCIAL AGREEMENT No. PVU-44 DATED 05.12.2024 UNDER PROJECT No. BG-RRP-2.017-0011 "ECOLOGICAL COLLABORATIVE ROBOTS POWERED BY GREEN HYDROGEN" UNDER THE RECOVERY AND SUSTAINABILITY MECHANISM FOR IMPLEMENTATION OF INVESTMENT UNDER C2I2 "INCREASING THE INNOVATION CAPACITY OF THE BULGARIAN ACADEMY OF SCIENCES (BAS) IN THE FIELD OF GREEN AND DIGITAL TECHNOLOGIES" FROM THE RECOVERY AND SUSTAINABILITY PLAN, BULGARIA.

REFERENCES

[1] Malik, M.; Camm, A.J.; Bigger, J.T.; Breithardt, G.; Cerutti, S.; Cohen, R.J.; Coumel, P.; Fallen, E.L.; Kennedy, H.L.; Kleiger, R.E.; et al. Heart rate variability. Standards of measurement, physiological interpretation, and clinical use. Eur. Heart J. 1996, 17, 354–381

[2] C.-K. Peng, S. Havlin, J. M. Hausdorff, J. E. Mietus, H. E. Stanley, and A. L. Goldberger, "Fractal mechanisms and heart rate dynamics: Long-range correlations and their breakdown with disease," Journal of Electrocardiology, vol. 28, suppl. 1, pp. 59–65, 1995, ISSN 0022-0736. doi:10.1016/S0022-0736(95)80017-4

[3] E. Gospodinova, P. Lebamovski, G. Georgieva-Tsaneva, G. Bogdanova, and D. Dimitrova, "Methods for mathematical analysis of simulated and real fractal processes with application in cardiology," Mathematics, vol. 10, no. 19, p. 3427, 2022. doi:10.3390/math10193427

[4] Hosking, J.R. Modeling persistence in hydrological time series using fractional differencing. Water Resour. Res. 1984, 20, 1898–1908.

[5] Brockwell, P.; Davis, R. Time Series: Theory and Methods, 2nd ed.; Springer: New York, NY, USA, 1991.

[6] Taqqu, M.; Willinger, W.; Sherman, R. Proof of a Fundamental Result in Self-Similar Traffic Modeling. Comput. Commun. Rev. 1997, 27, 5–23.

[7] van Roon, A.M.; Span, M.M.; Lefrandt, J.D.; Riese, H. Overview of Mathematical Relations Between Poincaré Plot Measures and Time and Frequency Domain Measures of Heart Rate Variability. Entropy 2025, 27, 861. https://doi.org/10.3390/e27080861

[8] Owis, M.I.; Abou-Zied, A.H.; Youssef, A.-B.M.; Kadah, Y.M. Study of features based on nonlinear dynamical modeling in ECG arrhythmia detection and classification. IEEE Trans. Biomed. Eng. 2002, 49, 733–736.

[9] Jauregui-Correa, J.C.; Morales-Velazquez, L. The Application of Recurrence Plots to Identify Nonlinear Responses Using Magnetometer Data for Wind Turbine Design. Machines 2025, 13, 233. https://doi.org/10.3390/machines13030233

[10] Zhu, H.; Jiang, N.; Xia, S.; Tong, J. Atrial Fibrillation Prediction Based on Recurrence Plot and ResNet. Sensors 2024, 24, 4978. https://doi.org/10.3390/s24154978

[11] Nayak, S.K.; Pradhan, B.; Mohanty, B.; Sivaraman, J.; Ray, S.S.; Wawrzyniak, J.; Jarzębski, M.; Pal, K. A Review of Methods and Applications for a Heart Rate Variability Analysis. Algorithms 2023, 16, 433. https://doi.org/10.3390/a16090433

[12] D'Addio, G.; Donisi, L.; Cesarelli, G.; Amitrano, F.; Coccia, A.; La Rovere, M.T.; Ricciardi, C. Extracting Features from Poincaré Plots to Distinguish Congestive Heart Failure Patients According to NYHA Classes. Bioengineering 2021, 8, 138. https://doi.org/10.3390/bioengineering8100138

[13] Zimatore, G.; Serantoni, C.; Gallotta, M.C.; Meucci, M.; Mourot, L.; Ferrari, D.; Baldari, C.; De Spirito, M.; Maulucci, G.; Guidetti, L. Recurrence Quantification Analysis Based Methodology in Automatic Aerobic Threshold Detection: Applicability and Accuracy across Age Groups, Exercise Protocols and Health Conditions. Appl. Sci. 2024, 14, 9216. https://doi.org/10.3390/app14209216